Available online at www.sciencedirect.com
ScienceDirect
Trans. Nonferrous Met. Soc. China 23(2013) 2071−2078
Transactions of Nonferrous Metals Society of China
www.tnmsc.cn

Mechanical alloying and subsequent heat treatment of Ag−Zn powders

Danny GUZMÁN[1], Oscar RIVERA[2], Claudio AGUILAR[3], Stella ORDOÑEZ[4], Carola MARTÍNEZ[4], Daniel SERAFINI[5], Paula ROJAS[6]

1. Department of Metallurgy, Atacama University and CRIDESAT, 485 Copayapu Avenue, Copiapó, Chile;
2. Department of Metallurgy, Atacama University, 485 Copayapu Avenue, Copiapó, Chile;
3. Department of Metallurgical and Materials Engineering, Federico Santa María Technical University, 1680 España Avenue, Valparaíso, Chile;
4. Department of Metallurgical Engineering, Santiago of Chile University, 3363 Bernardo O´Higgins Avenue, Santiago, Chile;
5. Department of Physics, Santiago of Chile University, 3363 Bernardo O´Higgins Avenue, Santiago, Chile;
6. School of Mechanical Engineering, Pontifical Catholic University of Valparaíso, 01567 Los Carreras Avenue, Quilpué, Chile

Received 6 September 2012; accepted 28 December 2012

Abstract: Microstructural evolution during mechanical alloying of Ag and Zn, and subsequent heat treatments were investigated. The mechanical alloying was carried out in a SPEX 8000D miller. The microstructural characterization was obtained by X-ray diffraction (XRD), transmission electron microscopy (TEM) and scanning electron microscopy (SEM). The thermal behavior was studied using differential scanning calorimetry (DSC). Based on the results obtained, it can be concluded that at the early stages of milling was possible to detect the ε, β, β', α solid solutions and remaining Zn. Later, the ε, β, β' and Zn phases disappeared while the Zn concentration of the α solid solution was strongly increased. After 7.2 ks of milling, the mechanical alloying process reached a steady state. During this period, both the composition and crystallite size of the α solid solution remained practically unchanged. On the other hand, subsequent heat treatments of milled powders showed that the α solid solution could also be obtained by the combination of mechanical alloying and heat treatment. Finally, the evolution of the microstructure during milling and annealing was combined to propose an optimal processing route in order to obtain a α solid solution.
Key words: mechanical alloying; Zn−Ag alloys; phase transformation; heat treatment

1 Introduction

Nowadays, the most electrical contact materials widely used in low and medium current applications (up to 100 A) are the Ag−CdO alloys [1]. Those alloys are obtained by internal oxidation of Ag−Cd alloys produced by casting [2]. Nevertheless, toxic Cd vapor is released into the environment during melting, service causing pollution and health problems [3]. For this reason, two instructions made by European Union, ROHS 2002/95/EC and WEEE 2002/96/EC have been implemented in 2006, which restricted the utilization of Cd in electronic and electric products of the European Union market.

The pollution-free Ag−SnO_2 alloy has been used to replace toxic Ag−CdO contact materials in the last two decades. However, SnO_2 has a higher thermal stability and it is more difficult to be wetted by liquid Ag than CdO [4]. Consequently, SnO_2 can be easily segregated to the surface. A further disadvantage of Ag−SnO_2 contact material compared with Ag−CdO is the lower safety against welding. The forces which are required to destroy the bridge weld are about double in comparison with Ag−CdO contacts [5]. Additionally, due to the high diffusion of the Sn atom during the internal oxidation of Ag−Sn alloys, an oxidized film on the surface is formed, avoiding a further progress of internal oxidation [6]. As a result, the internal oxidation of Sn is not completed especially when the content of Sn is more than about 5% of the Ag matrix.

Recently, Ag−ZnO alloys have aroused interest in

Corresponding author: Danny GUZMÁN; Tel: +56-52-206646; E-mail: danny.guzman@uda.cl
DOI: 10.1016/S1003-6326(13)62698-9

the technical field of contact materials as a replacement for the Ag−CdO alloys because the physical and chemical properties of Zn are similar to those of Cd and form a solid solution with Ag at the ambient temperature [7]. Furthermore, the electric resistance of Ag−ZnO (82% IACS) [8], is lower than that of Ag−SnO_2 (64% IACS) [9] and the wettability of ZnO by liquid Ag is better than the wettability of SnO_2 [10]. Additionally, VERMA et al [11] reported that Ag−ZnO alloys exhibit better arc erosion resistance and lower temperature rise compared with Ag−CdO and Ag−SnO_2 alloys. However, as for Ag−Sn alloys, when the amount of Zn in the alloy exceeds 5%, a layer of ZnO is formed on the surface of the material, and the selective oxidation of Zn still present in the internal layer does not proceed [12,13].

Nanocrystalline materials can be obtained by the mechanical alloying process which was developed by BENJAMIN [14]. Mechanical alloying is currently defined as solid-state powder processing technique of no-equilibrium involving repeated welding, fracturing, and rewelding of powder particles in a high energy ball mill [15]. By mechanical alloying, it is possible to obtain intermetallic compounds, amorphous alloys, over saturated solid solution, dispersion strengthened alloys and composite materials. Additionally, the mechanical alloying process increases the specific surface area, making the powder more reactive [15].

It is known that during the internal oxidation process, the diffusion rate of oxygen in the vicinity of the boundaries is larger than that through the crystalline grains, and the oxides tend to be precipitated at the boundaries of the silver crystalline grains as a result of reduced diffusion potential in the crystal [12].

Based on these arguments, it is proposed to study the internal oxidation of nanocrystalline α-Ag−Zn solid solution produced by mechanical alloying of Ag and Zn. It is expected that the nanocrystalline α solid solution will have microstructural and morphological characteristics that improve the kinetics of internal oxidation, increasing the conversion grade of Zn→ZnO and the oxide dispersion compared with other alloys of equal composition obtained by casting. In addition, as the nanocrystalline solid solution will be obtained in the form of fine powder, the oxygen diffusion distances will be reduced and consequently, the formation of the ZnO surface oxide layer can be avoided.

Due to the fact that there are no reports about the mechanical alloying in the Ag−Zn system, the objective of this work was to study the microstructural evolution during the milling of Ag and Zn, and subsequent heat treatment in order to propose an optimal obtaining route nanocrystalline α solid solution powders.

2 Experimental

The mechanical alloying process of 3.474 g Ag turnings (Sigma Aldrich, 99.9% purity) and 0.526 g Zn turnings (Merck, 99.9% purity) was carried out in a SPEX 8000D mill. The milling time employed was: 1.8, 2.7, 3.6, 7.2, 14.4 and 28.8 ks. In order to prevent agglomeration during the process, 0.040 g stearic acid was used. The millings were performed under Ar atmosphere (AGA Chile, 99.998% purity) using a ball-to-powder mass ratio of 20:1. The milling process was carried out in a discontinuous way: 3.6 ks of milling followed by 1.8 ks of rest.

The evolution of the phases during the mechanical alloying was studied by XRD using a Shimadzu XRD 6000, with Cu K_α radiation. The reticular parameters were calculated using the Cohen's method [16], while the crystallite sizes were obtained by the Scherrer's equation [16]. On the other hand, TEM characterization was carried out on a Fei Tecnail F20 equipment. The distribution of the phases was analyzed using SEM in a Jeol 5140 device equipped with an EDS analyzer. Before the SEM analyses, the milled powders were embedded in epoxy resin, grinded and polished. In order to determine the Fe contamination during the mechanical alloying process, some samples were analyzed by atomic absorption spectroscopy in a Varian SpectrAA−600 equipment.

The thermal behavior of the mechanical alloyed powder was studied by XRD and DSC in a DSC 2960 TA instruments device. The DSC analyses were carried out by flow of N_2 at a heating rate of 0.17 K/s.

3 Results and discussion

Figure 1(a) shows the XRD patterns of the samples obtained with different milling time. In order to observe the evolution of the phases during the mechanical alloying process, the XRD patterns were normalized in relation to the maximum intensity. It can be seen that during the first 1.8 ks of milling, it is possible to detect remaining Zn and α, ε, β, β' phases. The existence of α phase (FCC Ag-rich solid solution) was determined (Fig. 1(b)), which shows the variation of the Ag lattice parameter with respect to the milling time. It can be seen that during the first 1.8 ks of milling, the lattice parameter decreases from 0.4087 to 0.4084 nm. Considering that the size of the Zn atom (0.1332 nm) is smaller than Ag atom (0.1445 nm), the decrease of the Ag lattice parameter can be related with the entry of the Zn atom inside the Ag structure. On the other hand, the ε phase is a stable Ag−Zn solid solution, it has HCP

structure and its composition is 66%−89% Zn (mole fraction) [17], while β phase is an FCC Ag−Zn solid solution, which is stable above ~540 K and in a range of composition about 37% to 59% Zn. Upon a slow cooling, the β phase transforms to the complex hexagonal ζ phase. When the β phase is quenched at room temperature, the ζ phase is suppressed and the metastable cubic primitive β' phase is obtained [18]. The β' phase can be also obtained from the ζ phase by pressure [19]. The β and β' phases are metastable at room temperature. The metastable phases obtained during the mechanical alloying process can be understood considering the high energy transferred into powders and kinetic restrictions, which prevent the formation of more stable phases.

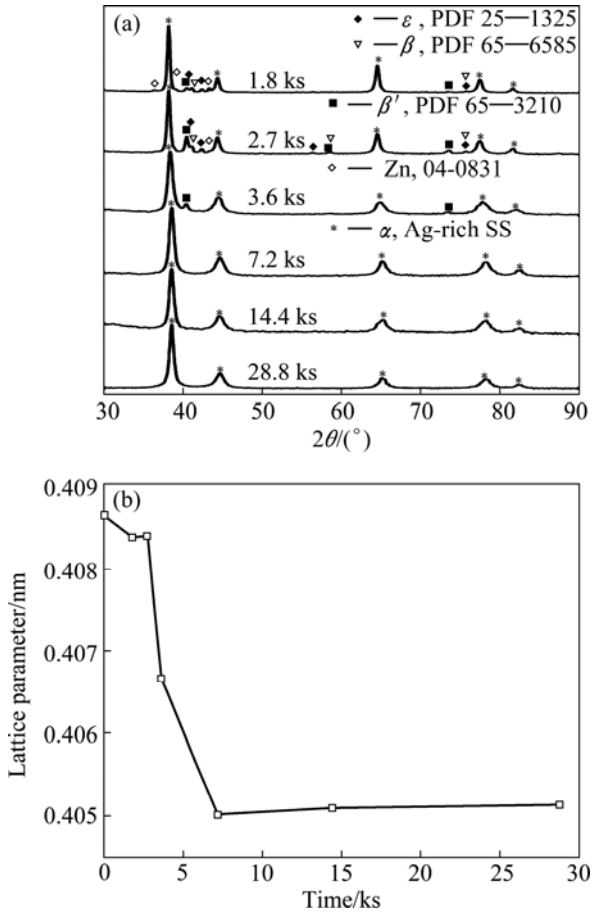

Fig. 1 XRD patterns of powders mechanically alloyed (a) and lattice parameter as function of milling time (b)

On the other hand, the η phase which is a Zn-rich solid solution was not detected. This observation is based on the Zn lattice parameters unchanged during the first 1.8 ks of milling. This suggests that during the mechanical alloying process the Zn atoms diffuse into the Ag structure, which is in agreement with the melting point difference between Zn and Ag.

Between 1.8 and 2.7 ks of milling, it is possible to observe an increase in the XRD intensity of the β, β' and ε phases, while the intensity of remaining Zn decreases. It is important to note that the β' is the phase which suffers a major increase in its XRD intensity during this period. As it can be seen in Fig. 1(b) between 1.8 and 2.7 ks, the lattice parameter of α phase remained unchanged. Based on this fact, it is possible to conclude that the decreased Zn is related principally with the β' phase increasing.

Between 2.7 and 3.6 ks of milling, the β' and α phases coexist. From the 7.2 ks of milling, only the α phase can be detected. This observation can be corroborated from Fig. 1(b), where it can be seen that between 2.7 and 7.2 ks of milling, the lattice parameter of the α phase decreased strongly, which is related with the disappearance of the β, ε and β' phases. After 7.2 ks, the α lattice parameter remained practically unchanged (0.4051 nm in average). This fact is an evidence that many of Zn atoms entered into the Ag structure. Based on the results obtained it can be concluded that it is possible to obtain α phase by mechanical alloying process. The following phase transformation sequence is proposed as $\text{Ag+Zn} \rightarrow \alpha+\text{Zn}+\beta+\beta'+\varepsilon \rightarrow \alpha+\beta' \rightarrow \alpha$.

Figure 2 shows the variation of the average crystallite size of α phase with respect to the time. It was calculated considering the (220) plane that during the first 7.2 ks the average crystallite size is rapidly reduced from 29 to 8 nm and the crystallite size approaches a minimum value. The minimum crystallite size is determined by the competition between the plastic deformation and dislocation motion that tends to decrease the grain size, and the recovery and recrystallization behaviors of the material tend to increase the grain size [20].

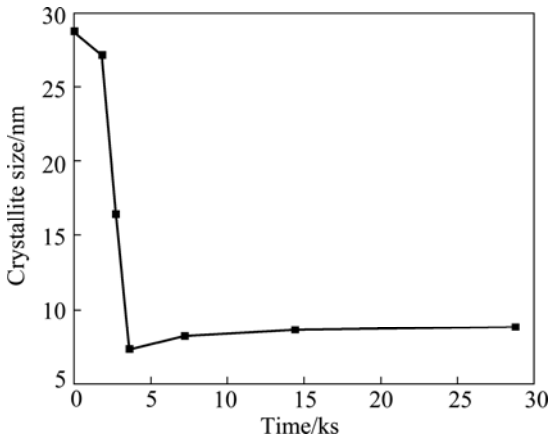

Fig. 2 Average crystallite size of α phase as function of milling time

In order to confirm the nanocrystalline nature of the α solid solution, a TEM study was carried out. Figure 3(a) shows the TEM image of powders milled for 7.2 ks. Figure 3(b) presents the dark field image with the

corresponding electron diffraction pattern. Based on the results obtained, it is possible to confirm that the sample is only composed of a nanocrystalline α solid solution with an average crystallite size of about 12 nm. The average crystallite size obtained from TEM was found to be greater than that calculated from XRD (8 nm). The results obtained using the Scherrer's method only represent an inferior limit of true crystallite size, because this equation does not contemplate the line broadening caused by the microstrain and the stacking faults.

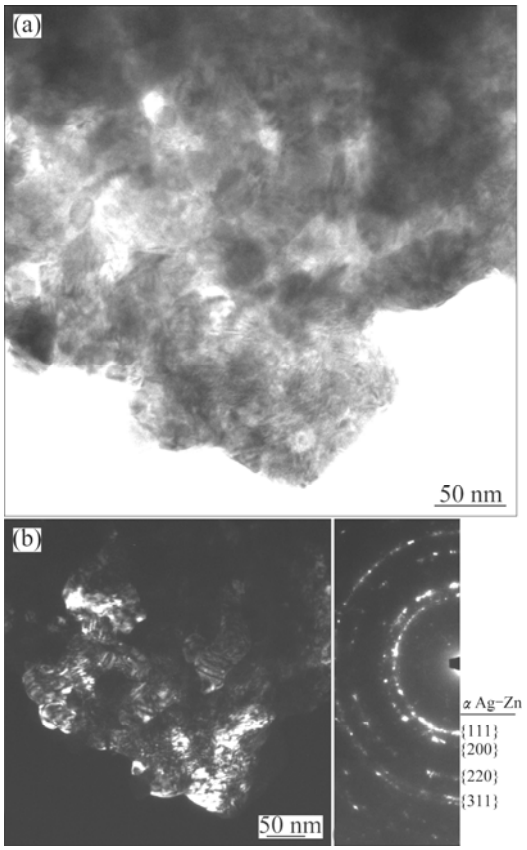

Fig. 3 TEM image of powders milled for 7.2 ks (a) and dark field image with corresponding electron diffraction pattern (b)

In order to observe the microstructural change during the milling, backscattered electron images (BSE) were taken from the cross-section of the milled powders. Figure 4(a) shows the microstructure in a cross-section of the powders obtained after 2.7 ks of milling. It also shows EDS analyses for two selected areas. It can be seen that the powders show a heavily deformed laminar structure, which is typical at the early stage of mechanical alloying process [15] and that the chemical composition, revealed by gray scale difference in BSE image, is quite heterogeneous. The Zn content (obtained by EDS analyses) ranged from 4.82% to 43.50%,. On the other hand, the cross-section micrographs taken from the powders milled for 7.2 (Fig. 4(b)) and 28.8 ks (Fig. 4(c)) show a much more homogeneous microstructure. The Zn content in the sample obtained after 28.8 ks of milling varied from 17.50% to 17.77% Zn. The BSE images confirmed the results obtained from XRD analysis. The loss of Zn could be explained that during the mechanical alloying process the ball and vial were covered with a thin layer of milled material, which apparently could be richer in Zn than Ag due to the major chemical interaction between the Zn and Fe atoms.

In order to determine the magnitude of Fe contamination, samples with 2.7, 7.2 and 28.8 ks of milling were analyzed using atomic absorption spectroscopy. The results showed that the Fe contamination was 0.237% in average. This fact confirms that the variation in the lattice parameter of the α phase was principally due to the entry of Zn atoms into Ag structure.

Figure 5 shows DSC curves of mechanically alloyed samples. It can be seen that between 372 and 503 K the sample milled for 1.8 ks shows an exothermic reaction coupled with an endothermic reaction. In the temperature ranging from 513 to 600 K, a second exothermic reaction coupled with a second endothermic reaction is detected.

In order to determine the nature of these reactions, a sample milled for 1.8 ks was heated up to 503 and 623 K and analyzed by XRD, respectively. The results can be observed in Fig. 6(a). In Fig. 6(a), sample without heat treatment is also shown. It is important to note that the composition of the α solid solution was determined using a mathematical relationship proposed by ABARCIA [21], which relates the lattice parameter with the α composition. Based on these results it can be concluded that during the first exothermic and endothermic reactions, the transformation of metastable β and β' phases into stable ζ takes place. During these reactions neither remaining Zn nor the α phase (1.2% Zn) suffers any changes. Based on the work of NOGUCHI [22], it is possible to establish that the second endothermic reaction is associated with the reversible transformation from ζ into β phase. On the other hand, during the second exothermic reaction the formation of the new α solid solution with a composition about 9.6% Zn takes place. This new α solid solution is produced due to the decrease of remaining Zn and ε phase.

For 2.7 ks of milling onwards, the first endothermic reaction is not detected. Based on the XRD results obtained from the samples heated up to 503 and 623 K (Fig. 6(b)), it is possible to conclude that during the first exothermic reaction, the β, β' and ε phases are transformed into stable ζ phase and a new α solid solution with a composition of 28.2% Zn, which coexists

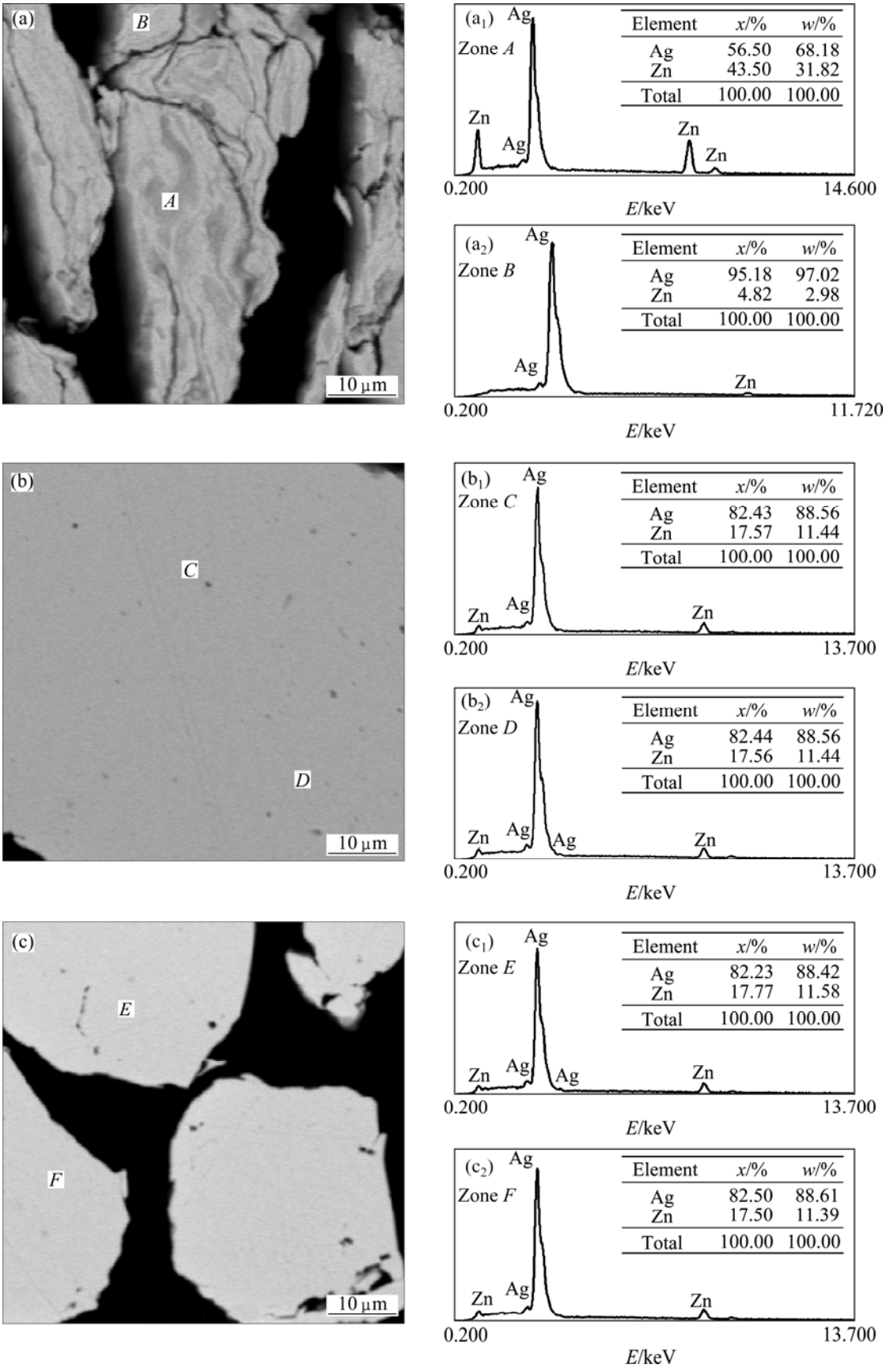

Fig. 4 BSE images of powders milled for 2.7 ks (a), 7.2 ks (b) and 28.8 ks (c), and corresponding EDS spectra for two selected areas

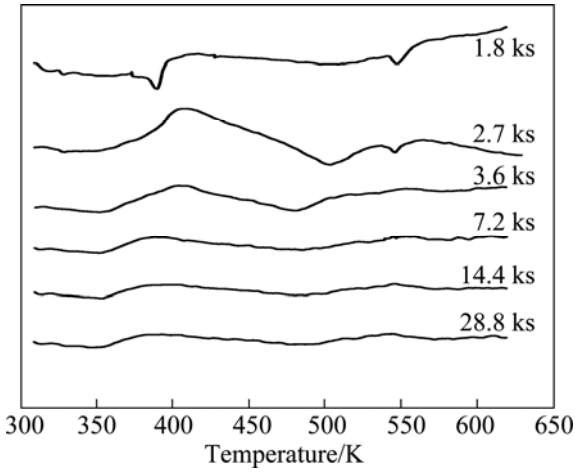

Fig. 5 DSC curves of mechanically alloyed samples

with the initial α solid solution (1.2% Zn). On the other hand, during the second exothermic event, the formation of α solid solution with a composition about 14.3% Zn takes place. After this reaction, it is possible to identify a little amount of remaining ζ phase.

From 3.6 ks of milling onwards, all the DSC traces show only two exothermic reactions. In order to determine the possibility to obtain a single-phase α alloy by mechanically alloying plus heat treatment, powders mechanically alloyed for 3.6 ks were heated up to 485 K and 623 K and analyzed by XRD. Figure 6(c) shows that after the heat treatment up to 485 K, it was only possible to detect the α phase by XRD. The calculated composition of the α solid solution was 13.3% Zn, which is lower than that obtained from the sample milled for 28.8 ks (18.0% Zn). The rest of Zn could be in the form of amorphous or nanocrystalline alloy with very small grain size, which cannot be detected. The absence of ζ phase can explain that the endothermic reaction about 547 K was not detected. After the second exothermic reaction, only α solid solution (a_o=0.4052 nm) with a composition about 17.8% Zn was detected, which is very close to that obtained from the sample milled for 28.8 ks. It is important to note that parallel to the transformation reactions, other processes like recovery and recrystallization are taking place. In this way, the average crystallite size calculated for the sample heated up to 623 K was 14 nm, which is greater than the one obtained from the sample mechanically alloyed for 3.6 ks (7 nm).

The production of single-phase α alloy by mechanical alloying plus heat treatment can be understood considering the decrease in diffusion path and the increase in the energy stored in the powders due to the microstructural refinement during the milling process (Fig. 2).

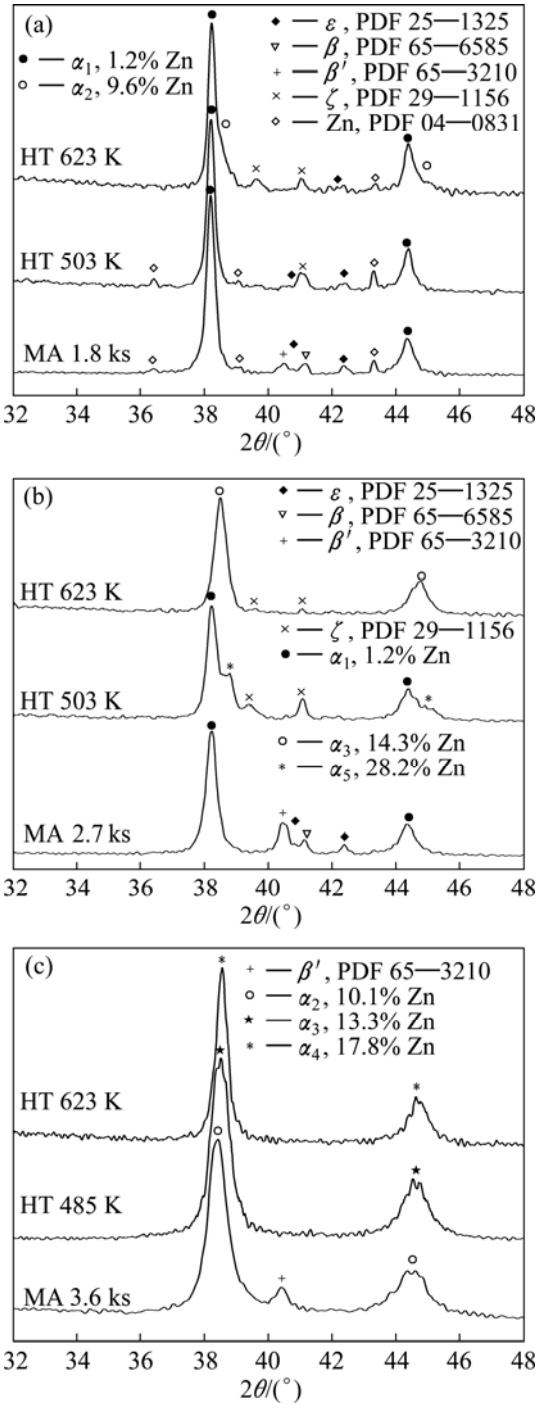

Fig. 6 XRD patterns of samples mechanically alloyed for 1.8 ks and heated up to 503 and 623 K (a), mechanically alloyed for 2.7 ks and heated up to 503 and 623 K (b) and mechanically alloyed for 3.6 ks and heated up to 485 and 623 K (c)

4 Conclusions

1) The microstructural evolution during mechanical alloying of Ag and Zn in mole ratio of 4:1 was analyzed. At the early stage, it was possible to detect the ε, β, β', α solid solutions and remaining Zn. Later, the ε, β, β' and Zn phases disappeared while the Zn concentration of the

α solid solution was strongly increased. At the later stage, the milling process reached a steady state. After 7.2 ks of milling, both the composition (≈18.0% Zn) and average crystallite size (8 nm) of the α phase remained practically unchanged. As a summary, the following phase reaction sequence was Ag+Zn$\rightarrow\alpha$+Zn+ β+β'+$\varepsilon\rightarrow\alpha$+$\beta'\rightarrow\alpha$.

2) The combination of mechanical alloying process and heat treatment was able to produce powders formed by single-phase α faster than mechanical alloying alone. The optimized processing route to obtain single-phase α alloy was found to be 3.6 ks of milling and the annealing at 623 K. This process produces α solid solution with a_o= 0.4052 nm, 17.8% Zn and with an average crystallite size of 14 nm.

Acknowledgements

The authors gratefully acknowledge “Fondo Nacional Desarrollo Científico y Tecnológico de Chile”, FONDECYT project Nº 11100284, for the economical support granted to the realization of this work. Additionally, the authors would like to thank Evelyn Cardenas for her time to improve the English of this paper.

References

[1] WOJTASIK K, MISSOL W. PM helps develop cadmium-free electrical contacts [J]. Metal Powder Report, 2004, 59(7): 34−39.

[2] KABAYAMA S, KAMIJYO E. Electric contact material and method of making the same: US3607244 [P]. 1971.

[3] WANG X, TIAN J. Health risks related to residential exposure to cadmium in Zhenhe county, China [J]. Archives of Environmental Health, 2004, 59(6): 324−330.

[4] MICHAL R, SAEGER K. Metallurgical aspects of silver-based contact materials for air-break switching devices for power engineering [J]. IEEE Transactions on Components, Hybrids, and Manufacturing Technology, 1989, 12(1): 71−81.

[5] BOHM W, WOLMER R, SZULCZYK A, MALIKOWSKI W. Material for electrical contacts: US4341556 [P]. 1982.

[6] TANAKA S, HIRATA T, YIDA M. Method of making Ag−SnO_2 contact materials by high pressure internal oxidation: US5078810 [P]. 1992.

[7] BAKER H. Alloys phase diagrams [M]. Vol. 3. USA: ASM International, 1997.

[8] JOSHI P, RAO V, REHANI B, PRATAB A. Silver−zinc oxide electrical contact materials by mechanochemical synthesis route [J]. Indian Journal of Pure and Applied Physics, 2007, 45(1): 9−15.

[9] PANDEY A, VERMA P, PANDEY O P. Comparison of properties of silver−tin oxide electrical contact materials through different processing routes [J]. Indian Journal of Engineering and Materials Sciences, 2008, 15(3): 236−240.

[10] NAKAMURA T, SAKAGUCHI O, KUSAMORI H, MATSUZAWA O, TAKAHASHI M, YAMAMOTO T. Method for preparing Ag−ZnO electric contact material and electric contact material produced thereby: US6432157 B1 [P]. 2002.

[11] VERMA P, PANDEY O P, VERMA A. Influence of metal oxides on the arc erosion behavior of silver metal oxides electrical contact materials [J]. Journal of Materials Science & Technology, 2004, 20(1): 49−52.

[12] SHIBATA A. Silver-metal oxide composite and method of manufacturing the same: US3933486 [P]. 1976.

[13] SATOH M, HIJIKATA M, MAEDA H, MORIMOTO I. Electrical contact material of silver base alloy: US4131458 [P]. 1978.

[14] BENJAMIN J S. Dispersion strengthened superalloys by mechanical alloying [J]. Metallurgical Transactions, 1970, 1: 2943−2951.

[15] SURYANARAYANA C. Mechanical alloying and milling [M]. USA: Marcel Dekker, 2004.

[16] CULLITY D. Elements of X-ray diffraction [M]. USA: Addison-Wesley Publishing Company Inc, 1956.

[17] GÓMEZ-ACEBO T, SUNDMAN B. Modelización termodinámica de las aleaciones Ag−Zn [J]. Revista de Metalurgia, 1998, 34: 262−266.

[18] ORR R L, ROVEL J. Thermodynamics of the structural modifications of AgZn [J]. Acta Metallurgica, 1962, 10(10): 935−939.

[19] IWASAKI H, FUJIMURA T, ICHIKAWA M, ENDO S, WAKATSUKI M. Pressure-induced phase transformation in AgZn [J]. Journal of Physics and Chemistry of Solids, 1985, 46(4): 463−468.

[20] ECKER J, HOLZER J C, KRILL C E III, JOHNSON W L. Structural and thermodynamic properties of nanocrystalline FCC metals prepared by mechanical attrition [J]. Journal of Materials Research, 1992, 7(7): 1751−1761.

[21] ABARCIA J. Estudio de la Producción de Aleaciones Ag−Zn mediante aleado mecánico y tratamiento térmico [D]. Chile: Metallurgical Engineering Thesis of the Atacama University, 2011.

[22] NOGUCHI S. An experimental study on the stability of the ζ phase in the silver zinc system [J]. Journal of the Physical Society of Japan. 1962, 17(12): 1844−1856.

Ag−Zn 粉末的机械合金化和随后的热处理

Danny GUZMÁN[1], Oscar RIVERA[2], Claudio AGUILAR[3], Stella ORDOÑEZ[4],
Carola MARTÍNEZ[4], Daniel SERAFINI[5], Paula ROJAS[6]

1. Department of Metallurgy, Atacama University and CRIDESAT, 485 Copayapu Avenue, Copiapó, Chile;
2. Department of Metallurgy, Atacama University, 485 Copayapu Avenue, Copiapó, Chile;
3. Department of Metallurgical and Materials Engineering,
Federico Santa María Technical University, 1680 España Avenue, Valparaíso, Chile;
4. Department of Metallurgical Engineering, Santiago of Chile University,
3363 Bernardo O´Higgins Avenue, Santiago, Chile;
5. Department of Physics, Santiago of Chile University, 3363 Bernardo O´Higgins Avenue, Santiago, Chile;
6. School of Mechanical Engineering, Pontifical Catholic University of Valparaíso,
01567 Los Carreras Avenue, Quilpué, Chile

摘　要：研究了在机械合金化过程中 Ag 和 Zn 以及随后的热处理中的显微组织演变。机械合金化在 SPEX 8000D 铣床中进行。采用 X 射线衍射(XRD)、透射电子显微镜(TEM)和扫描电子显微镜(SEM)观察样品的显微组织。使用差示扫描量热计(DSC)研究样品的热性能。结果表明，在合金化初期的碾磨过程中能观察到 ε, β, β', α 固溶体和剩余的 Zn。随后，ε, β, β' 和 Zn 相消失，α 固溶体中的 Zn 浓度剧烈升高。在碾磨 7.2 ks 后，机械合金化过程达到稳定状态。在此期间，α 固溶体的组分和晶粒尺寸保持不变。后续热处理表明 α 固溶体也能够通过机械合金化结合热处理得到。最后，为了得到 α 固溶体，根据碾磨和热处理过程中样品的微观组织演变，提出一个最佳的工艺路线。

关键词：机械合金化；Zn−Ag 合金；相变；热处理

(Edited by Xiang-qun LI)